

Probing Protein Shelf Lives from Inverse Mean First Passage Times

Vishal Singh and Parbati Biswas*

Department of Chemistry, University of Delhi, Delhi-110007

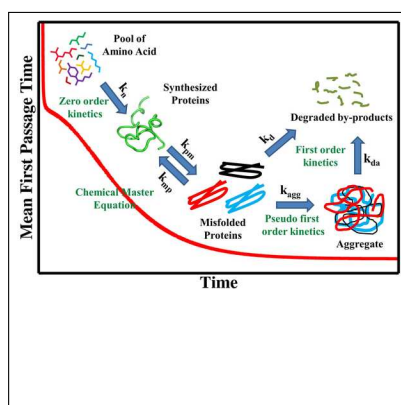
E-mail: pbiswas@chemistry.du.ac.in

Phone: +91-11-2766-6646

Abstract

Protein aggregation is investigated theoretically via protein turnover, misfolding, aggregation and degradation. The Mean First Passage Time (MFPT) of aggregation is evaluated within the framework of Chemical Master Equation (CME) and pseudo first order kinetics with appropriate boundary conditions. The rate constants of aggregation of different proteins are calculated from the inverse MFPT, which show an excellent match with the experimentally reported rate constants and those extracted from the ThT/ThS fluorescence data. Protein aggregation is found to be practically independent of the number of contacts and the critical number of misfolded contacts. The age of appearance of aggregation-related diseases is obtained from the survival probability and the MFPT results, which matches with those reported in the literature. The calculated survival probability is in good agreement with the only available clinical data for Parkinson's disease.

Graphical TOC Entry



Keywords

Protein Turnover, Aggregation, Chemical Master Equation, Mean First Passage Time, Survival Probability

Most proteins have been evolved to spontaneously fold to their native states, which determine their functional specificity and diversity.^{1,2} Any phenotypic or genotypic variations may induce abnormal amino acid modifications and cause protein misfolding.³⁻⁵ Misfolded proteins disrupt normal cellular functions and may be potentially toxic.⁶ The spontaneous self-assembly of misfolded proteins often lead to the formation of aggregates, which are associated with a wide variety of debilitating disorders like Alzheimer's, Parkinson's, Creutzfeldt-Jakob's, Huntington's, Amyotrophic lateral sclerosis (ALS) and dementia.^{2,7-9} The Protein Quality Control (PQC) system present in the cell manages these misfolded proteins and helps them to either refold back to their respective native conformations via chaperones or degrades them to amino acids and eventually replaces them with their newly synthesized replicas.^{10,11} This phenomenon known as protein turnover, is a highly specific and precisely regulated process that involves a constant renewal of the functional proteins by allowing the damaged or non-functional ones to be eliminated from the cell.¹⁰

The underlying link among protein folding, misfolding, aggregation and degradation equilibria implies that a change in any one of these components would directly/indirectly affect the others.¹² External factors like aging, genetic mutation, oxidative stress, pH and temperature results in the failure of the protein turnover process and leads to the formation of aggregates/fibrils.^{13,14} These aggregates are typically highly organized hydrogen-bonded structures that are more stable compared to the native protein,^{6,7} kinetically-trapped in the lowest free energy state. Thus once formed such aggregates are extremely stable for long time periods and acts as a nucleus for further propagation.

This work analyzes the folding outcome of a protein through protein turnover followed by misfolding, aggregation and degradation. The rate of formation of proteins from the amino acids follows a zero-order kinetics,^{15,16} which is an input for the subsequent $P \rightleftharpoons M$ equilibrium, that is governed by the time evolution of the misfolded contacts. The Chemical Master Equation (CME) for this equilibria is derived from the splitting probabilities of the misfolded contacts at a particular time instant. The misfolded proteins self-associate to form

aggregates as described by a first order differential equation. The Mean First Passage Time (MFPT) required for the protein to form aggregates from the misfolded proteins is calculated from both CME and the first order differential equation under appropriate boundary conditions. The rate constants of aggregation of different disease causing proteins are evaluated from the inverse MFPT, which show an excellent match with the experimentally reported rate constants¹⁷⁻²² and those extracted from the ThT/ThS fluorescence data. The age of appearance of these diseases are directly evaluated from the MFPT and the survival probability results, which agrees well with those reported in literature. The survival probability result is in good agreement with the only available clinical data for Parkinson's disease.²³

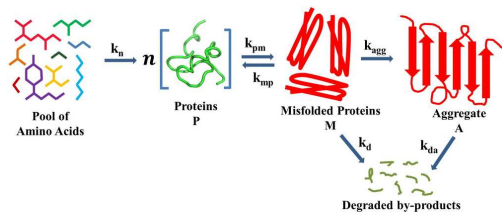


Figure 1: Schematic diagram of protein turnover followed by misfolding, aggregation and degradation.

Figure 1 depicts a schematic diagram of the life cycle of a protein. Protein synthesis begins from a pool of amino acids via protein turnover.²⁴ The synthesized native proteins may misfold and the misfolded proteins subsequently self assemble to form aggregates.^{8,10,12} Both misfolded proteins and aggregates may degrade to by-products, which is eliminated from the system.¹⁰ The misfolded state represents the ensemble of misfolded proteins, where each one is characterized by a critical number of misfolded contacts, q_{MC} . For a given protein, all chains in the native conformational ensemble are assumed to be of equal lengths with equal number of contacts that are in equilibrium with the misfolded state.

The number of proteins, n , present at time t may be calculated assuming zero order kinetics^{15,16} with the rate constant k_n . The solution of this rate equation is $n = k_n t$. The total number of contacts present at time t is given by: $q(t) = n_P n = n_P k_n t$, where n_P is the number of contacts present in each protein.

The number of misfolded contacts present in the native protein at time $t + \Delta t$ is $q_M(t)$. The protein acquires a misfolded conformation M at time t_M when the number of misfolded contacts reaches a critical value, q_{MC} . The rate of increase/decrease of a misfolded contact at an infinitesimal time interval, Δt , may be given by

$$\text{rate}(q_M(t) \rightarrow q_M(t) + 1) = W(q_M(t) + 1, q_M(t)) = q(t) k_{pm}$$

and
$$\text{rate}(q_M(t) \rightarrow q_M(t) - 1) = W(q_M(t) - 1, q_M(t)) = q_M(t) k_{mp}$$

where, k_{pm} denotes the rate constant for the conversion of a native contact into a misfolded one, while k_{mp} is the rate constant for the backward reaction. The transition probabilities for the gain and loss of a misfolded contact at time Δt are represented as $W(q_M(t) + 1, q_M(t))\Delta t$ and $W(q_M(t) - 1, q_M(t))\Delta t$ respectively. Thus the probability to remain in a given misfolded state with $q_M(t)$ misfolded contacts at time Δt is $1 - W(q_M(t) + 1, q_M(t))\Delta t - W(q_M(t) - 1, q_M(t))\Delta t$.²⁵ Thus the probability, $P(M, t_M | q_M, t)$ to acquire the misfolded conformation, M , at time t_M may be expressed as a difference equation.^{25,26}

$$\begin{aligned} P(M, t_M + \Delta t | q_M, t) &= W(q_M(t) + 1, q_M(t))\Delta t P(M, t_M | q_M(t) + 1, t + \Delta t) \\ &\quad + W(q_M(t) - 1, q_M(t))\Delta t P(M, t_M | q_M(t) - 1, t + \Delta t) \quad (1) \\ &+ [1 - W(q_M(t) + 1, q_M(t))\Delta t - W(q_M(t) - 1, q_M(t))\Delta t] P(M, t_M | q_M, t) \end{aligned}$$

The Chemical Master Equation (CME)^{25,27-29} for the native conformational ensemble may be obtained from Eqn (1) in the limit $\Delta t \rightarrow 0$ as

$$\sum_{i=1}^n \frac{dP_i(M, t_M | q_M, t)}{dt_M} = \sum_{i=1}^n \sum_{q_M' = q_M(t) - 1}^{q_M(t) + 1} W(q_M', q_M(t)) P_i(M, t_M | q_M', t) \quad (2)$$

The probability $P(M, t_M | q_M, t)$ follows the reflecting boundary condition for the number of misfolded contacts, $q_M(t) < q_{MC}$. The MFPT may be obtained from Eqn (2) as (refer to

the Supporting Information (SI))

$$-n = W(q_M(t)+1, q_M(t)) \sum_{i=1}^n [\tau_i(q_M+1) - \tau_i(q_M)] + W(q_M(t)-1, q_M(t)) \sum_{i=1}^n [\tau_i(q_M-1) - \tau_i(q_M)] \quad (3)$$

The equation^{25,29} holds true for all values of $q_M(t)$ ranging from 1 to q_{MC} . Since $\tau(0) = 0$ and $\tau(q_{MC} + 1)$ is not required, this equation may be solved to obtain the MFPT, τ_M , of the misfolded proteins in terms of the Gauss hypergeometric function ${}_2F_1(\alpha, \beta; \gamma; z)$ (refer to SI).

$$\tau_M = \sum_{i=1}^n \tau_i(q_M) = \frac{n}{k_{pm}} \sum_{j=q_M(t)}^{q_{MC}} \frac{1}{[q(t) - (j - 1)]} [{}_2F_1(-j, 1; q(t) - (j - 2); -r)] \quad (4)$$

where $r = k_{mp}/k_{pm} < 1$.³⁰ The generalized equation of MFPT is simplified using the integral identity as²⁶

$$\tau_M = \frac{n}{k_{pm}} \int_0^1 (1-x)^{q(t)-q_{MC}-q_M(t)} \frac{[(1-x)^{q_M(t)}(1+rx)^{1+q_{MC}} - (1-x)^{1+q_{MC}}(1+rx)^{q_M(t)}]}{(1+r)x} dx \quad (5)$$

Degradation of the misfolded proteins follow first order kinetics.^{15,16,31} The rate equation for degradation may be defined in terms of the evolution of $q_M(t)$ with time as: $\frac{dq_M(t)}{dt} = -k_d q_M(t)$, where k_d is the rate constant for the degradation of misfolded proteins calculated from the half-life³¹ of a protein as, $k_d = 0.693/t_{1/2}$. This first order differential equation may be solved as

$$q_M(t) = \exp(-k_d t) = \exp\left(-\frac{0.693}{t_{1/2}} t\right) \quad (6)$$

Protein aggregation may be viewed as the self-assembly of misfolded proteins.^{17,32} The rate equation for aggregation followed by degradation of the aggregates is given by (refer to SI)

$$\frac{dn_{A_s}(t)}{dt} = k_{agg} n_M - k_{da} n_{A_s}(t) \quad (7)$$

where, n_{A_s} and n_M are the number of aggregates and the number of misfolded proteins

present in an aggregate respectively. The ratio R is defined as $R = n_{A_s}/n_M$. k_{agg} denotes the pseudo first order aggregation rate constant, whereas k_{da} is the degradation rate constant of the aggregates. Eqn (7) may be solved by using absorbing boundary condition defined by

$$n_{A_s}(t) = \begin{cases} n_{A_s}; & t = \tau_{agg}; \quad \text{absorbing boundary condition} \\ 0; & t = \tau_M \end{cases}$$

The solution of Eqn (7) is given for n_{A_s} as

$$n_{A_s} = \frac{n_M k_{agg}}{k_{da}} [1 - e^{-(\tau_{agg} - \tau_M)k_{da}}] \quad (8)$$

The time required for the aggregation of misfolded proteins, τ_{agg} , may be obtained by rearranging Eqn (8) as

$$\tau_{agg} = \frac{1}{k_{da}} \log \left[\frac{e^{k_{da}\tau_M}}{1 - \frac{n_{A_s} k_{da}}{n_M k_{agg}}} \right] = \frac{1}{k_{da}} \log \left[\frac{e^{k_{da}\tau_M}}{1 - RK} \right] \quad (9)$$

where the ratio of rate constants, K is defined as $K = k_{da}/k_{agg}$. Thus the MFPT of aggregation may be expressed as

$$\begin{aligned} \tau_A &= \tau_M + \tau_{agg} \\ \tau_A &= \frac{n}{k_{pm}} \int_0^1 (1-x)^{n_P k_n t - q_{MC} - e^{-k_d t}} \\ &\quad \frac{[(1-x)^{e^{-k_d t}} (1+rx)^{1+q_{MC}} - (1-x)^{1+q_{MC}} (1+rx)^{e^{-k_d t}}]}{(1+r)x} dx + \frac{1}{k_{da}} \log \left[\frac{e^{k_{da}\tau_M}}{1 - \frac{n_{A_s} k_{da}}{n_M k_{agg}}} \right] \end{aligned} \quad (10)$$

Figures 2(a) and 2(b) portray the MFPT of the selected proteins (refer to Table S1 of SI for the selection of proteins) for specified values of $k_{da} = 10^{-3}k_{agg}$ for $n_M = 5$ and $n_M = 8$ respectively. The value of R is fixed for each protein. The MFPT displays an initial high value that decreases exponentially with time (refer to the inset) with an increase in the number of proteins. The MFPT decreases monotonically as the turnover of proteins increase

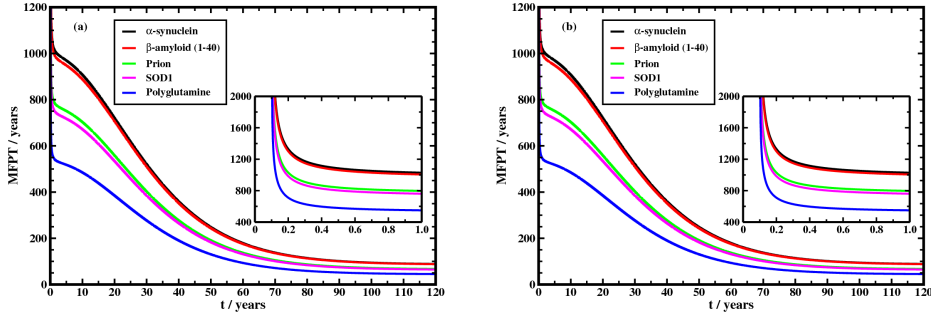


Figure 2: MFPT of the aggregate with different numbers of misfolded proteins present in an aggregate (a) $n_M = 5$ (b) $n_M = 8$ for the selected proteins. The MFPT's are calculated from their respective literature values of reported rate constants^{17–22,26,33} and half-lives^{34–40} for a specified value of the rate constant $k_{da} = 10^{-3}k_{agg}$. Inset figure depicts the MFPT at initial times.

with time followed by the formation of aggregates. The MFPT of each protein reaches a plateau with time marking the age of appearance of the aggregation-related diseases. The MFPT of the selected proteins are calculated from Eqn (10) using the respective values of the reported rate constants^{17–22,26,33} and half-lives^{34–40} as listed in Table 1.

The MFPT of the aggregate remains constant for fixed values of R for a given n_{A_s} . This affirms that protein aggregation is independent of the number of aggregates, n_{A_s} for fixed values of k_n , k_{pm} , k_{mp} , k_{agg} , $t_{1/2}$ and R . To the best of our knowledge there are no reported literature values of the rate constants or half-lives for the degradation of aggregates. The rate of degradation of these aggregates is much slower compared to the rate of their formation, as the aggregated proteins are very stable.^{6,7} For the given range of $K = 10^{-1} - 10^{-5}$, the values of R are tuned to match the MFPT with the age of appearance of aggregation-related diseases as given in S2 of SI. The rate constant of aggregation is proportional to the inverse MFPT, which may be calculated as

$$k_{agg} = C \times \frac{1}{MFPT} \quad (11)$$

where C is the proportionality constant equal to R . Thus, Eqn (11) is recast as

$$k_{agg} = R \times \frac{1}{MFPT} \quad (12)$$

Table 1 displays the values of MFPT of the selected proteins by varying K and R . Table 1 also shows a comparison between the calculated and experimental values of the rate constants of aggregation of these proteins. The calculated values of k_{agg} show an excellent match with the rate constants extracted from the ThT/ThS fluorescence data (refer to Figures S1(a), (b) and (c) of SI) and those obtained from experiments.¹⁷⁻²²

Protein aggregation is found to be practically independent of the number of contacts (n_P) and the critical number of misfolded contacts (q_{MC}) (refer to SI). The MFPT is independent of the rate constant, k_{mp} for fixed values of k_n , k_{pm} and k_{agg} .²⁶ The survival probability is calculated by assuming that the distribution of proteins in the conformational ensemble is Gaussian²⁶ at time t . The average number of proteins at an infinitesimal time interval Δt may be estimated as

$$\mu(t) = n - [nk_{pm}\Delta t - (k_d\Delta t + k_{agg}\Delta t)k_{mp}\Delta t] \quad (13)$$

The survival probability of the proteins is given by

$$S_{n(t)} = \sum_{i=1}^n \frac{1}{\sqrt{2\pi\sigma^2}} e^{-\frac{(i-\mu(t))^2}{2\sigma^2}} \quad (14)$$

where σ^2 is the variance of the Gaussian distribution.

Table 1: MFPT of the selected proteins (calculated from Eqn (10)) and a comparison of the experimentally obtained rate constants of aggregation, k_{agg} with those calculated from our theory for $k_{mp}^{26} = 10^{-12} s^{-1}$.

Proteins (Length)	Diseases	$k_n = 0.17h^{-1}$ (³³)			$K = 10^{-3}, n_M = 5$			$K = 10^{-4}, n_M = 5$		
		k_{pm}^{26} (s^{-1})	$t_{1/2}^{34-40}$ (h)	k_{agg}^{18-22} (h^{-1}) (Experimental)	R	MFPT (years)	k_{agg} (h^{-1}) (calculated)	R	MFPT (years)	k_{agg} (h^{-1}) (calculated)
β -amyloid (1-40)	Alzheimer's	$10^{-9.96}$	9	8×10^{-6}	6	85.87	7.9×10^{-6}	6	85.64	8.0×10^{-6}
β -amyloid (1-42)	Alzheimer's	$10^{-9.96}$	9	2×10^{-5}	15	86.27	1.9×10^{-5}	15	85.68	2.0×10^{-5}
α -synuclein (1-140)	Parkinson's	$10^{-9.97}$	16.8	4×10^{-5}	30	86.93	3.9×10^{-5}	30.6	87.46	4.0×10^{-5}
Prion (23-230)	Prion	$10^{-9.86}$	24	1×10^{-4}	56	65.79	0.9×10^{-4}	57	65.25	1.0×10^{-4}
Polyglutamine (1-47)	Huntington's	$10^{-9.70}$	24	1×10^{-3}	320	44.03	0.8×10^{-3}	380	44.22	1.0×10^{-3}
Tau* (1-441)	Alzheimer's	$10^{-9.96}$	12	1.2×10^{-3}	600	87.17	0.8×10^{-3}	880	87.63	1.1×10^{-3}
SOD1* (1-154)	ALS	$10^{-9.84}$	381	2.5×10^{-3}	750	63.30	1.4×10^{-3}	1300	63.59	2.3×10^{-3}
IAPP* (1-37)	Type II diabetes	$10^{-9.70}$	0.3	7.5×10^{-3}	950	45.60	2.4×10^{-3}	2600	45.80	6.5×10^{-3}

*for tau, SOD1 (superoxide dismutase 1) and IAPP (islet amyloid polypeptide precursor or amylin) proteins, the rate constant of aggregation is extracted from the experimental ThS/ThT fluorescence data and fitted to the Finke-Watzky equation^{17,41} (refer to Figures S1(a), (b) and (c) of SI respectively).

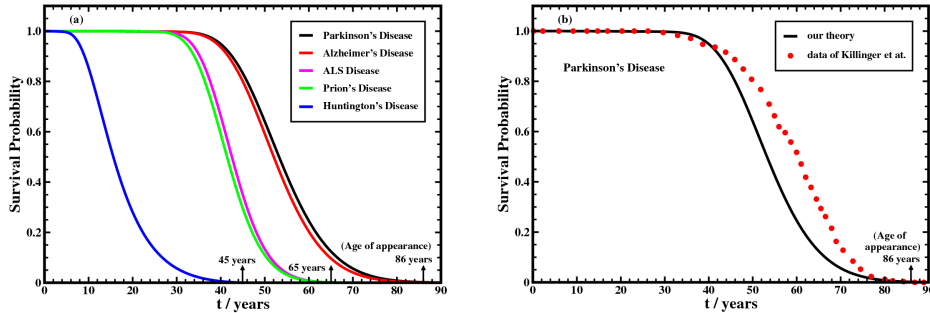


Figure 3: (a) Survival probability of selected proteins for $k_{mp}=10^{-12}s^{-1}$ and their respective values of the reported rate constants^{17–22,26,33} and half-lives^{34–40} and (b) a comparison of the survival probability from our theory with the available clinical data of Killinger et al.²³ for Parkinson's disease.

Figure 3(a) shows the survival probability of the selected aggregation-prone proteins for reported values of the rate constants^{17–22,26,33} and half-lives.^{34–40} All proteins are initially present in their respective native states. Thus, the survival probability of these proteins shows a maximum that remains constant upto a threshold time, after which it exhibits a slow decrease with time due to the initiation of misfolding. The survival probability decreases monotonically with time and reaches zero after a long time, marking the formation of aggregates. The zero value of the survival probability corresponds to the age of appearance of the aggregation-related diseases. Figure 3(b) displays a comparison of the survival probability obtained from our theory with the only available clinical data of Killinger et al.²³ for Parkinson's disease. The calculated survival probability is in good agreement with this clinical data.²³ Table 2 provides a comparison of the age of appearance of the aggregation-related diseases from our results of MFPT and survival probability with the respective values reported in the literature.

In this work, protein aggregation is investigated theoretically via protein turnover, misfolding, aggregation and degradation. The rate of formation of proteins in turnover follows a zero-order kinetics, which is used in the $P \rightleftharpoons M$ equilibrium, that is governed by time evolution of the misfolded contacts. The Chemical Master Equation for this equilibria is derived from the splitting probabilities of the misfolded contacts at a particular instant of

Table 2: Comparison of the age of appearance of diseases calculated from the results of MFPT and survival probability along with their reported literature values.

Diseases	Age of appearance (in years)		
	MFPT from Eqn (10)	Surv. prob. from Eqn (14)	Literature
Alzheimer's ^{9,42}	85.87	87	≥ 85
Parkinson's ⁴³	86.93	86	85 – 89
Prion ³⁶	65.79	65	55 – 75
ALS ⁴²	63.30	64	50 – 70
Huntington's ²²	44.03	45	30 – 50
Type II diabetes ⁴⁴	45.60	46	45 – 64

time. Self-association of the misfolded proteins to form aggregates follows pseudo first order kinetics. The Mean First Passage Time (MFPT) of aggregation for the selected proteins is estimated from the CME and the pseudo first order kinetics with appropriate boundary conditions. The MFPT of aggregation is found to be practically independent of the number of contacts and the critical number of the misfolded contacts. The rate constants of aggregation of different proteins are calculated from the inverse MFPT, which show an excellent match with the experimentally reported rate constants and those extracted from the ThT/ThS fluorescence data. The age of appearance of aggregation-related diseases are directly evaluated from the MFPT and the survival probability. The survival probability result is in good agreement with the only available clinical data for Parkinson's disease.

Supporting Information Available

Mathematical derivation of MFPT and it's solution; Calculation of the aggregation rate equation; Selection of proteins; Calculation of the aggregation rate constants; Variation of the values of K with the values of R ; MFPT of the aggregate of β -amyloid with varying n_P and q_{MC} . This material is available free of charge via the Internet at <http://pubs.acs.org/>.

Corresponding Author:

*E-mail: pbiswas@chemistry.du.ac.in

Conflict of Interest:

The authors declare no conflict of interest.

Acknowledgement

The authors gratefully acknowledge DST-SERB, INDIA (EMR/2016/006619) for financial support. V. Singh acknowledges CSIR, India for providing financial assistance in the form of SRF (09/045(1410)/2016-EMR-I).

References

- (1) Dill, K. A.; MacCallum, J. L. The protein-folding problem, 50 years on. *science* **2012**, *338*, 1042–1046.
- (2) Dobson, C. M. Protein folding and misfolding. *Nature* **2003**, *426*, 884–890.
- (3) Kumar, A.; Biswas, P. Effect of Correlated Pair Mutations in Protein Misfolding. *J. Phys. Chem. B* **2019**, *123*, 5069–5078.
- (4) Kumar, A.; Biswas, P. Effect of site-directed point mutations on protein misfolding: A simulation study. *Proteins Struct. Funct. Bioinf.* **2019**, *87*, 760–773.
- (5) Baruah, A.; Biswas, P. The role of site-directed point mutations in protein misfolding. *Phys. Chem. Chem. Phys.* **2014**, *16*, 13964–13973.
- (6) Gregersen, N.; Bross, P.; Vang, S.; Christensen, J. H. Protein misfolding and human disease. *Annu. Rev. Genomics Hum. Genet.* **2006**, *7*, 103–124.
- (7) Chiti, F.; Dobson, C. M. Protein misfolding, functional amyloid, and human disease. *Annu. Rev. Biochem.* **2006**, *75*, 333–366.

- (8) Knowles, T. P.; Vendruscolo, M.; Dobson, C. M. The amyloid state and its association with protein misfolding diseases. *Nat. Rev. Mol. Cell Biol.* **2014**, *15*, 384–396.
- (9) Pedersen, J. T.; Heegaard, N. H. Analysis of protein aggregation in neurodegenerative disease. *Anal. Chem.* **2013**, *85*, 4215–4227.
- (10) Goldberg, A. L. Protein degradation and protection against misfolded or damaged proteins. *Nature* **2003**, *426*, 895–899.
- (11) Toyama, B. H.; Hetzer, M. W. Protein homeostasis: live long, won't prosper. *Nat. Rev. Mol. Cell Biol.* **2013**, *14*, 55–61.
- (12) Enam, C.; Geffen, Y.; Ravid, T.; Gardner, R. G. Protein Quality Control Degradation in the Nucleus. *Annu. Rev. Biochem.* **2018**, *87*, 725–749.
- (13) Chi, E. Y.; Krishnan, S.; Randolph, T. W.; Carpenter, J. F. Physical stability of proteins in aqueous solution: mechanism and driving forces in nonnative protein aggregation. *Pharm. Res.* **2003**, *20*, 1325–1336.
- (14) Wang, W.; Nema, S.; Teagarden, D. Protein aggregation-Pathways and influencing factors. *Int. J. Pharm.* **2010**, *390*, 89–99.
- (15) Rothman, S. How is the balance between protein synthesis and degradation achieved? *Theor. Biol. Med. Modell.* **2010**, *7*, 25.
- (16) Hargrove, J. L.; Hulsey, M. G.; Beale, E. G. The kinetics of mammalian gene expression. *Bioessays* **1991**, *13*, 667–674.
- (17) Morris, A. M.; Watzky, M. A.; Agar, J. N.; Finke, R. G. Fitting neurological protein aggregation kinetic data via a 2-step, minimal/"Ockham's Razor" model: The Finke-Watzky mechanism of nucleation followed by autocatalytic surface growth. *Biochemistry* **2008**, *47*, 2413–2427.

- (18) Bieschke, J.; Zhang, Q.; Powers, E. T.; Lerner, R. A.; Kelly, J. W. Oxidative metabolites accelerate Alzheimer’s amyloidogenesis by a two-step mechanism, eliminating the requirement for nucleation. *Biochemistry* **2005**, *44*, 4977–4983.
- (19) Fink, A. L. The aggregation and fibrillation of α -synuclein. *Acc. Chem. Res.* **2006**, *39*, 628–634.
- (20) Watzky, M. A.; Morris, A. M.; Ross, E. D.; Finke, R. G. Fitting yeast and mammalian prion aggregation kinetic data with the Finke-Watzky two-step model of nucleation and autocatalytic growth. *Biochemistry* **2008**, *47*, 10790–10800.
- (21) Baskakov, I. V.; Bocharova, O. V. In vitro conversion of mammalian prion protein into amyloid fibrils displays unusual features. *Biochemistry* **2005**, *44*, 2339–2348.
- (22) Chen, S.; Ferrone, F. A.; Wetzel, R. Huntington’s disease age-of-onset linked to polyglutamine aggregation nucleation. *Proc. Natl. Acad. Sci. U.S.A.* **2002**, *99*, 11884–11889.
- (23) Killinger, B. A.; Madaj, Z.; Sikora, J. W.; Rey, N.; Haas, A. J.; Vepa, Y.; Lindqvist, D.; Chen, H.; Thomas, P. M.; Brundin, P. et al. The vermiform appendix impacts the risk of developing Parkinson’s disease. *Sci. Transl. Med.* **2018**, *10*, eaar5280.
- (24) Newsholme, E.; Leech, A. *Functional biochemistry in health and disease*; John Wiley & Sons, 2011.
- (25) van Kampen, N. G. *Stochastic processes in physics and chemistry*; Elsevier, 1992; Vol. 1.
- (26) Singh, V.; Biswas, P. Estimating the mean first passage time of protein misfolding. *Phys. Chem. Chem. Phys.* **2018**, *20*, 5692–5698.
- (27) Munsky, B.; Khammash, M. The finite state projection algorithm for the solution of the chemical master equation. *J. Chem. Phys.* **2006**, *124*, 044104.
- (28) Gillespie, D. T. Exact stochastic simulation of coupled chemical reactions. *J. Phys. Chem.* **1977**, *81*, 2340–2361.

- (29) Gardiner, C. W. *Handbook of stochastic methods*; Springer Berlin, 1985; Vol. 3.
- (30) Thirumalai, D.; Woodson, S. Kinetics of folding of proteins and RNA. *Acc. Chem. Res.* **1996**, *29*, 433–439.
- (31) Eden, E.; Geva-Zatorsky, N.; Issaeva, I.; Cohen, A.; Dekel, E.; Danon, T.; Cohen, L.; Mayo, A.; Alon, U. Proteome half-life dynamics in living human cells. *Science* **2011**, *331*, 764–768.
- (32) Morris, A. M.; Watzky, M. A.; Finke, R. G. Protein aggregation kinetics, mechanism, and curve-fitting: a review of the literature. *Biochim. Biophys. Acta* **2009**, *1794*, 375.
- (33) Smeets, J. S.; Horstman, A. M.; Schijns, O. E.; Dings, J. T.; Hoogland, G.; Gijzen, A. P.; Goessens, J. P.; Bouwman, F. G.; Wodzig, W. K.; Mariman, E. C. et al. Brain tissue plasticity: protein synthesis rates of the human brain. *Brain* **2018**, *141*, 1122–1129.
- (34) Patterson, B. W.; Elbert, D. L.; Mawuenyega, K. G.; Kasten, T.; Ovod, V.; Ma, S.; Xiong, C.; Chott, R.; Yarasheski, K.; Sigurdson, W. et al. Age and amyloid effects on human central nervous system amyloid-beta kinetics. *Ann. Neurol.* **2015**, *78*, 439–453.
- (35) Cuervo, A. M.; Stefanis, L.; Fredenburg, R.; Lansbury, P. T.; Sulzer, D. Impaired degradation of mutant α -synuclein by chaperone-mediated autophagy. *Science* **2004**, *305*, 1292–1295.
- (36) Harris, D. A. Cellular biology of prion diseases. *Clin. Microbiol. Rev.* **1999**, *12*, 429–444.
- (37) Crisp, M. J.; Mawuenyega, K. G.; Patterson, B. W.; Reddy, N. C.; Chott, R.; Self, W. K.; Weihl, C. C.; Jockel-Balsarotti, J.; Varadhachary, A. S.; Buccelli, R. C. et al. In vivo kinetic approach reveals slow SOD1 turnover in the CNS. *J. Clin. Invest.* **2015**, *125*, 2772–2780.
- (38) Persichetti, F.; Carlee, L.; Faber, P. W.; McNeil, S. M.; Ambrose, C. M.; Srinidhi, J.;

- Anderson, M.; Barnes, G. T.; Gusella, J. F.; MacDonald, M. E. Differential expression of normal and mutant Huntington's disease gene alleles. *Neurobiol. Dis.* **1996**, *3*, 183.
- (39) David, D. C.; Layfield, R.; Serpell, L.; Narain, Y.; Goedert, M.; Spillantini, M. G. Proteasomal degradation of tau protein. *J. Neurochem.* **2002**, *83*, 176–185.
- (40) Young, A. Central nervous system and other effects. *Adv. Pharmacol.* **2005**, *52*, 281.
- (41) Watzky, M. A.; Finke, R. G. Transition metal nanocluster formation kinetic and mechanistic studies. A new mechanism when hydrogen is the reductant: slow, continuous nucleation and fast autocatalytic surface growth. *J. Am. Chem. Soc.* **1997**, *119*, 10382–10400.
- (42) Shaw, C. A. *Neural Dynamics of Neurological Disease*; John Wiley & Sons, 2017.
- (43) Rodriguez, M.; Rodriguez-Sabate, C.; Morales, I.; Sanchez, A.; Sabate, M. Parkinson's disease as a result of aging. *Aging cell* **2015**, *14*, 293–308.
- (44) Wu, Y.; Ding, Y.; Tanaka, Y.; Zhang, W. Risk factors contributing to type 2 diabetes and recent advances in the treatment and prevention. *Int. J. Med. Sci.* **2014**, *11*, 1185–1200.